Traitement du Signal
Vol. 41, No. 6, December, 2024, pp. 2777-2795
Journal homepage: http://iieta.org/journals/ts

An Effective Prediction Model of Myocardial Infarction Using Convolution Kernel Weight Based Convolutional Neural Network

P. Saranya[1*], C. Vennila[2]

[1] Department of Computer Science and Engineering, Government College of Engineering Srirangam, Tiruchirappalli 620012, Tamilnadu, India
[2] Department of Electronics and Communication Engineering, VSB Engineering College, Karur 639111, Tamilnadu, India

Corresponding Author Email: saranyap@gces.edu.in

https://doi.org/10.18280/ts.410602

Received: 11 March 2024
Revised: 16 July 2024
Accepted: 28 August 2024
Available online: 31 December 2024

Keywords:
electrocardiogram (ECG), morphology, Principal Component Analysis (PCA), Fuzzy Weight Particle Swarm Optimization (FWPSO), algorithm, Convolution Kernel Weight Based CNN (CKWCNN)

ABSTRACT

One of the frequent cardiac conditions brought on by persistent myocardial ischemic is myocardial infarction (MI), generally referred as a heart attack. The clinical standard for treating individuals with this disease is made possible by the electrocardiogram (ECG), which allows for the earlier and precise diagnosis of MI. It is significant for patients with MI to automatically detect using ECG signals. De-noising is a critical step in signal processing. In this work, Empirical Mode Decomposition (EMD) uses a repetitive process known as sifted to calculate the basic functions that represent the signal as an extension of signal-dependent basic functions. Sifting process, a deconstruction procedure, is used to dynamically divide noisy data into inherent oscillatory parts understood as Intrinsic Mode Functions (IMFs). EMD, The IMFs are optimized using the Fuzzy Weight Particle Swarm Optimization (FWPSO) algorithm. Furthermore, we have acquired morphological features from the P-QRS-T waveforms and extracted characteristics of ECG segments using Principal Component Analysis (PCA) from the preferred ECG area. Finally, Convolution Kernel Weight Based CNN (CKWCNN) classifier is used to improve the functionality and outcomes of automated diagnostics. We obtained the ECG data from the Physikalisch-Technische Bundesanstalt's (PTB) database. We then evaluate the detection techniques using metrics such as accuracy, F-measure, sensitivity, and precision. We tested the MI detection and classification methods using the PTB dataset. Fivefold cross validation is applied to the PTB dataset to separate training sets and testing sets.

1. INTRODUCTION

Globally, cardiovascular disease (CVD) is the primary cause of mortality, accounting for 31% of all fatalities each year. The number of reported CVD deaths is increasing, with 17.9 million deaths occurring annually [1, 2]. By 2030, it is anticipated that there will be more than 23.6 million CVD deaths annually because of the rapidly rising prevalence of diabetes, obesity, and other cardiovascular-related risk factors. (Acute) Myocardial infarctions account for the largest proportion of mortality among CVD in the United States and other nations. In the US, an MI affects one person every 40 years on average. Methods that use electrocardiogram (ECG) readings in conjunction with machine learning to identify abnormalities in the signal and, by extension, abnormalities associated with certain illnesses are included here [3].

By monitoring the potential bioelectric fluctuation of the human heart, an electrocardiogram (ECG) signal may identify abnormal states and malfunctions [4]. ECG signals present a difficult challenge when it comes to making an accurate diagnosis of the clinical state that they represent. Human MI diagnosis and identification take time and are not accurate. Therefore, before proposing a specific course of therapy, cardiologists must precisely forecast and identify the appropriate form of irregular cardiac ECG waves [5, 6]. For this, hour-long ECG recordings that need to be watched and analyzed may be necessary.

Because it is inexpensive and noninvasive, ECG is often used for clinical diagnosis. The absence of several comprehensive, publicly accessible datasets with a lengthy history of real-world ECG readings, as well as machine learning techniques with high precision (>89%) and a wide range of options, have presented difficulties [7]. Over the course of the most recent few years, a great number of different algorithms for detecting myocardial infarction (MI) have been presented. The four main steps in the implementation of these algorithms were denoising, segmentation, feature extraction, and MI classification. However, the heartbeat segmentation detector is essential for MI classification because mistakes made during ECG heartbeat identification might affect the final classification findings. The identification of the P-QRS-T waves is the primary component of the heartbeat segmentation process. However, the majority of methods include a preprocessing stage to obtain the signal ready. There are multiple noise levels in this form of the signal. When an ECG signal is acquired and transmitted, the noise is polluted. This makes manual and automated ECG signal analysis very difficult, and noise may be mistaken for abnormal cardiac problems [8]. Therefore, noise-free ECG readings are required for accurate cardiac diagnosis.

Manual ECG performance requires domain knowledge and is subject to interobserver fluctuations. In some cases, medical expertise such as emergency paramedics in remote locations may not be physically available. This has prompted more research into the use of ECG signals in computer-assisted myocardial infarction diagnosis using artificial intelligence (AI). Deep learning (DL) and feature extraction are two types of AI algorithms. On the other hand, the latter is fully automated and has gained popularity because of its convenience, reliable performance, and ability to train on large data sets.

The Empirical Mode Decomposition (EMD) is decomposing non-stationary signals into a series of Intrinsic Mode Functions (IMFs) [9]. Convolutional neural networks (CNNs), in particular, have recently received much attention for their use in forecasting MI and atrial fibrillation, which has limited the potential of alternative algorithms to perform better on deadlier acute myocardial infarction.

Existing research has presented several methods for autonomous detection and localization of MI. These methods include wavelet transform techniques, time-domain approaches, polynomial fitting methods, and supervised machine learning algorithms. Although these strategies have shown promise, they still face significant challenges in clinical applications. For instance, segmenting the heart to assess strain is a complex and labor-intensive process. In addition, the intricate spatiotemporal motion of the heart can lead to difficulties in its implementation. DL models have made rapid progress in recent years across a wide range of research fields, particularly in cardiac segmentation. Numerous studies have focused on detecting myocardial infarction (MI) using DL approaches; however, they still face significant challenges. One major issue is inadequate image preprocessing, which is required for DL models to accurately extract features. Another significant limitation is the scarcity of large high-quality datasets.

This study proposes the development of an automated detection approach for acute myocardial infarction with CKWCNN to address the limitations of previous research. This model presents notable advantages for predicting MI compared with other DL approaches. The CKWCNN is distinguished by its ability to autonomously learn intricate patterns and characteristics from ECG signals, which are essential for the early detection of myocardial infarction. Its convolutional layers effectively capture both local and global dependencies in ECG data. In contrast to conventional ML methods that depend on manual feature extraction, CKWCNN independently learns representations from the raw data. This reduces the necessity for specialized knowledge and increases adaptability to different datasets and conditions. Additionally, the CKWCNN's efficient parameter utilization and regularization methods enhance the model's generalization, ensuring consistent performance across various patient groups and healthcare environments. Overall, CKWCNN distinguishes itself in predicting myocardial infarction by utilizing its strengths in feature learning, spatial representation, and performance optimization, positioning it as a valuable tool for improving clinical decision-making and patient outcomes in cardiology.

Accurate denoising, identification, and categorization of cardiac arrhythmias has been suggested using a unique approach. The first approach for signal denoising is called Empirical Mode Decomposition with Fuzzy Weight Particle Swarm Optimization (EMD-FWPSO). The ECG waveform is then divided into P-QRS-T waves. The characteristics and outcomes of the automated diagnostics were then used for the Convolution Kernel Weight-Based CNN (CKWCNN) classifier. This method combines classification and feature extraction processes, automatically classifies single-lead myocardial infarction ECGs, and performs an extensive analysis.

The primary objective of the research work is listed as follows:

- The PTB dataset is a well-known benchmark dataset that has been used to analyze the efficiency of the CKWCNN approach and compare it with other existing classical models.
- In the preprocessing stage, Empirical Mode Decomposition with Fuzzy Weight Particle Swarm Optimization (EMD-FWPSO) is presented. The IMFs are optimized using the Fuzzy Weight Particle Swarm Optimization (FWPSO) algorithm. This simplifies the model, reduces the impact of noise on the electrocardiogram signal, and allows for faster diagnosis in clinical practice.
- In the segmentation stage, electrocardiogram segment characteristics are derived from the chosen electrocardiogram section using PCA, and morphological features are extracted from P-QRS-T waves.
- In the classification stage, a Convolution Kernel Weight-Based CNN (CKWCNN) classifier was utilized to classify the electrocardiogram signal to identify the myocardial infarction.
- MATLAB was used to implement the proposed CKWCNN. Compared with existing algorithms, the proposed CKWCNN algorithm has the highest precision, recall, specificity, accuracy, and F1 scoring performance.

The remainder of this study is structured as follows. Section II offers a concise summary of the relevant literature. Section III presents the major contents of the proposed algorithm. Section IV delineates the experimental outcomes and discussion. Finally, Section V concludes the study.

2. LITERATURE SURVEY

Sraitih et al. [10] evaluated an automated ECG MI detection system's resilience and endurance across diverse noise sources. The proposed method seeks to categorize myocardial infarction (MI) and normal (NOR) states by using authentic electrocardiogram (ECG) recordings from the PTB database. This procedure encompasses data preparation and segmentation and employs an innovative framework to differentiate between patient data and noise using the MIT-BI Noise Stress Testing Database (NSTDB). The methodology encompasses three supervised machine-learning models: Support Vector Machine (SVM), Random Forest (RF), and k-nearest neighbors (KNN). Performance indicators, including the accuracy, precision, recall, and F1 score, were used to evaluate the effectiveness of the models.

Tripathy et al. [11] presented multi resolution ECG research was used to identify MI pathophysiology. The FBSE-EWT method was utilized to deconstruct the 12-lead ECG data across many timescales. This technique produces nine sub-band ECG signals for each lead, and is subsequently examined for kurtosis, skewness, and entropy. The proposed algorithm yielded 99.74% reliability, 99.87% sensitivity, and 99.60% precision for detecting MI. The proposed strategy improves the MI identification efficiency by 3% over wavelet-based characteristics.

Baloglu et al. [12] suggested a DL model for the diagnosis of MI, and it had an end-to-end structure. The model was applied to conventional 12-lead ECG data. When applied to all ECG lead signals, the CNN algorithm combined with the suggested framework produced an amazing recall and accuracy performance of over 99.00%.

Sridhar et al. [13] implemented an analysis on the ECGs of two hundred different participants (52 normal and 148 MI). The suggested approach begins with the pre-processing of signals and then continues with the identification of R peaks using the Pan-Tompkins algorithm. The focus has been on extracting nonlinear characteristics. The extracted features were arranged using t-test, and the rankings were used as inputs for the Probabilistic Neural Network (PNN), SVM, Decision Tree (DT), and KNN classifiers. These classifiers were used to differentiate between healthy and abnormal classes. Using the SVM classifier, this approach produced the highest accuracy (97.96%) for MI and specificity (98.89%).

Jahmunah et al. [14] suggested automatic categorization of ECG data into regular, CAD, MI, and CHF groups utilizing CNN and GaborCNN models. The unbalanced database is then weighed. The CNN and aborCNN models had a categorization accuracy rate of over 98.5% for usual, CVD and MI. The utilizing of the aboabor CNN to automatically classify ECG signals. Our approach may be verified with a larger dataset and can help physicians screen for CVDs using electrocardiogram signals.

Fatimah et al. [15] devised two automated MI diagnosis systems utilizing a single-channel ECG data. The basic approach detects MI using ECG beats, whereas the updated technique uses 4096 samples. The Fourier decomposition technique (FDM) removes the power line interference from ECG beats/frames (FIBFs). The main algorithms that use the kNN classifier have the greatest accuracy, sensitivity, and selectivity. The new method avoids beat extraction and utilizes FDM only once for noise reduction and FIBF extraction. It exhibits 99% accuracy, 99.61% sensitivity, and 99.73% selectivity.

Kapfo et al. [16] described a technique called variation mode decomposition as a means of extracting prediction information about MI from the signal of an ECG. Features were discerned, and principal components were obtained from multiscale covariance matrices. The effectiveness of the collected characteristics for the identification and categorization of MI and regular is evaluated with the help of the k-nearest neighbor and support vector machine classifiers. The suggested approach was successful in achieving an efficiency of 99.88%, with a precision of 99.90% and a sensitivity of 99.88%.

Cho et al. [17] created an AI program based on DL was and proven to diagnose MI using a 6-lead ECG. A variation autoencoder (VAE) was created using 412,461 ECGs, and a limb 6-lead ECG was employed to reconstruct the ECG. We used data from 9,536, 1,301, and 1,768 electrocardiograms of adult patients. The proposed method has an area under the transmitter operating characteristic curves of 0.880 for evaluation and 0.854 after external testing.

Kayikcioglu et al. [18] suggested a technique for classifying ST segments depending on characteristics derived from multi-lead ECG data utilizing time-frequency distributions information. The suggested technique, in contrast to most other research in the existing body of research, is built on a four-class categorization system and is evaluated on a large dataset comprising three distinct datasets: MIT-BIH Arrhythmia information, Long-Term ST data, and the European ST-T database system. Employing Choi-Williams time-frequency distribution characteristics, the weighted k-NN method had the best average efficiency amongst the categorization algorithms, with correctness of 94.23%, sensitive of 95.72%, and precision of 98.15%. This was accomplished using Choi and Williams.

Zhao et al. [19] developed 667 STEMI ECGs and 7571 control electrocardiograms were utilized for AI-based STEMI auto diagnostic method. The system is a 12-lead standard ECG diagnostic system that uses artificial intelligence. It could provide useful information for future improvements in ECGs, especially for conditions that require multilead ECG evaluation, such as ischemic heart disease and premature beats. Ventricular pathology and hypertrophy. The algorithm's sensitivity (recall), selectivity, correctness, and clarity in a comparison test with cardiologists were 90%, 98%, 94%, 97.82%, and 0.9375, respectively. It also had an AUC of 0.9740 (95% CI, 0.9419–and a score of F1.

Hammad et al. [20] suggested a new ML-based DL approach for diagnosing MI and CD in PTB-XL ECG data, the CD and MI signals were assigned to a DL algorithm to obtain deep features. Furthermore, a novel activation function that can quickly converge to a normal activation function was suggested. When CNN and SVM classifiers were used to extract features, the overall accuracy of the method improved to 99.20%.

Rai and Chatterjee [21] introduced an automated system, incorporating convolutional neural networks (CNN), a hybrid CNN-Long Short-Term Memory (LSTM) network, to identify the most effective model. The method is used in two steps: (i) the original unbalanced dataset is used and (ii) the Synthetic Minority Oversampling Technique (SMOTE) data sampling algorithm is used to create a balanced dataset.

Han et al. [22] proposed a comprehensible approach for MI localization and seriousness forecasts based on 12 leads. First, the ontology structure of the intelligent MI diagnosis knowledge graph was established. The entity metric values, such as the QRS complex, T wave, and ST segment pulsation morphology, were then obtained using a DenseNet network-based method and diagnostic rules. Production rules are also used to explain MI diagnoses. Finally, all pertinent experiments are conducted and validated using high-quality ECG databases. The sensitivity, accuracy, specificity, and mean F1 value for forecasting the severity period of patients with MI were 94.86%, 93.65%, 97.76%, and 94.27%, respectively.

Muraki et al. [23] proposed an automatic prediction model for acute MI in ECG using CNN and LSTM. The cardiac cycle of the left ventricle was fed into CNN and VGG16 for feature extraction. Subsequently, LSTM classifies instances as healthy or acute MI. The long-axis left ventricle image had 85.1% classification accuracy, while the short-axis view had 83.2% classification accuracy.

Mirza et al. [24] presented a framework for predicting MI using 15-lead ECG signals. This study helps to improve the effectiveness of classifying ten MI classes and standard classes.

The suggested 1D-CNN architecture produced average sensitivity, accuracy, precision, specificity, and F1-scores of 99.91%, 99.98%, 99.91%, 99.99%, and 99.91%, respectively, on the PTB dataset. According to the evaluation results, the suggested 1D-CNN structure will offer greater efficiency in identifying MI attacks. Table 1 presents a summary of the existing MI detection techniques.

2.1 Problem statement

The main disadvantage of the existing models is their inability to be interpreted. The internal processes and functions of the models are incomprehensible, as is the logic behind predictions. Recent studies using deep learning algorithms to diagnose myocardial infarction (MI) have rarely described prediction methods. This lack of transparency makes doctors wary of adopting these models in clinical decision-making. To fill this gap, we created and compared deep-learning algorithms for MI classification to increase comprehension and application. Despite extensive research on the diagnosis of myocardial infarction, some details need to be considered. Most studies typically focus on a single ECG lead; however, it is important to consider all available leads. Utilizing a 12-lead ECG recording is aligned with the true principles of MI diagnosis. Additionally, there has been limited research evaluating and weighing the significance of each lead in the diagnosis of myocardial infarction. Some authors evaluate all 12 leads simultaneously; however, each lead contains unique and complementary information that requires separate processing. Finally, a few PTB dataset researchers examined interpatient scenarios. Given the variations among individual patients, the inter-patient protocol is closely tied to real-world clinical practice and application. Intra-patient protocols, conversely, need to demonstrate the model's feasibility and suitability and may even result in an overly optimistic detection. To address these gaps, we propose a novel and practical framework for medical-grade MI detection and localization.

Table 1. Summary of the existing MI detection techniques

Reference	Algorithm	Advantages	Disadvantages
[10]	SVM, KNN, and random forest (RF)	ECG tools for MI detection.	Large dataset training necessitates a substantial amount of computational resources.
[11]	SVM	Compared to wavelet characteristics, the suggested method improves accuracy by over 3%.	It necessitates significant computational resources and expertise.
[12]	CNN	The proposed model can detect MI with excellent performance, making it suitable for use in wearable devices and intensive care units.	It may be difficult to ensure consistent performance of the proposed model across different MI datasets of varying sizes and characteristics.
[13]	K-NN, DT, SVM, and PNN	The system can be used in real-time to detect anomalies related to MIs.	This method is restricted to a small dataset. Additionally, manually extracting and selecting features can be time-consuming.
[14]	convolutional neural network (CNN) and unique GaborCNN	The GaborCNN model is capable of classifying additional ECG classes with optimal classification performance.	Few CAD and CHF patients were included in the intended study. GaborCNN training and testing require a larger dataset.
[17]	VAE	12-lead ECG and a portable 6-lead ECG device.	Its reliance on the assumption of Gaussian distribution in latent space may not always be appropriate for complex medical data such as ECG signals.
[18]	weighted k-NN	The method as two-class approaches.	In the proposed study, the large data size, and dimensionality of the feature space can lead to longer processing times and higher resource requirements for classification tasks.
[19]	AI-based STEMI	The proposed algorithm could significantly enhance the existing STEMI systems globally.	The proposed method depends on specific ECG changes that may not be observed in all patients, potentially resulting in misdiagnosis.
[20]	CNN, SVM	When using CNN and SVM classifiers for feature extraction, the overall accuracy of the method increases to 99.20%.	A significant drawback of the proposed algorithm is its reliance on large labelled datasets, which can be challenging to acquire in clinical environments, increasing the risk of overfitting.
[21]	CNN-LSTM	The unique data balancing technique resolves imbalanced data and significantly increases minority class accuracy.	A limitation of the proposed algorithm is its inability to assess the severity of myocardial infarction and identify the affected region, which restricts its diagnostic effectiveness.
[22]	DenseNet	The accuracy, sensitivity, specificity, and average F1 score for predicting the severity period of MI patients were 93.65%, 94.86%, 97.76%, and 94.27%, respectively.	A limitation of the proposed method is its significant computational demands, which may result in longer training times and higher resource requirements.
[23]	CNN and LSTM	This suggests that echocardiography can identify myocardial infarction.	It was prone to overfitting because of the model's complexity, especially when trained on small datasets.
[24]	1D-CNN	Based on evaluation results, the 1D-CNN design should increase MI event detection efficiency.	Its limited capacity to capture spatial dependencies.

3. PROPOSED METHODOLOGY

Initially, the input ECG data are acquired from the PTB database. Next, the image was preprocessed and filtered. The approach for signal noise removal used in this study is called Empirical Mode Decomposition with Fuzzy Weight Particle Swarm Optimization (EMD-FWPSO). IMFs' energy of the IMFs and Eigen period are used to produce EMD, Intrinsic Mode Functions (IMFs), which are performed using FWPSO. The clustering approach can identify the borders between IMFs with reduced sounds, high-frequency noise, and meaningful data. In addition, segmentation is performed with QRS complex detection, which improves segmentation accuracy.

Next, the features were mined using PCA. The QRS complex and P and T waves were detected to execute the heartbeat separation detectors. Third, ECG segmentation characteristics were obtained from the chosen ECG segment utilizing PCA. Finally, this selected feature is given to the CKWCNN classifier for classification, which gives the severity of the myocardial infarction. Finally, the results were evaluated using the performance evaluation metrics. Figure 1 shows the flowchart of the proposed MI categorization approach. Preprocessing, signal segmentation, feature extraction, categorization, and effectiveness assessment are the five processes that constitute this procedure.

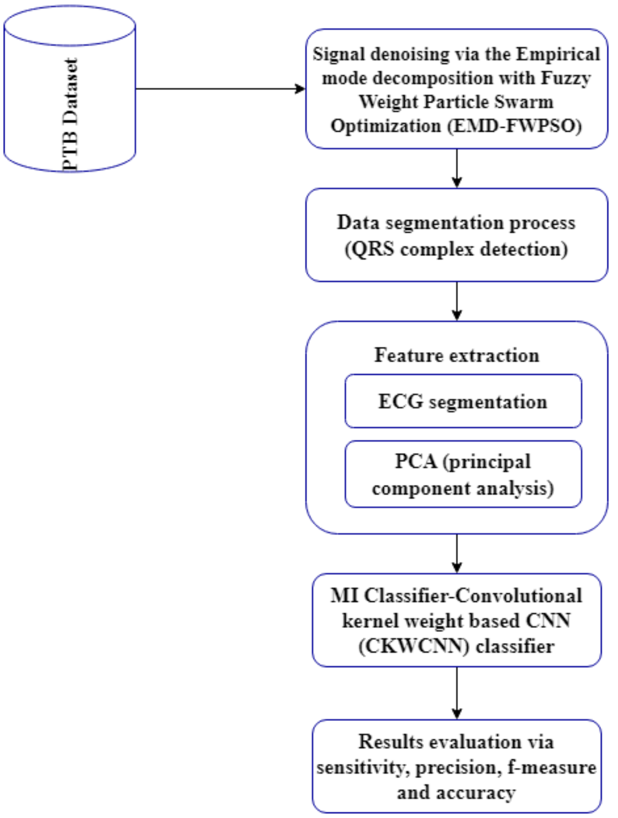

Figure 1. Flowchart diagram of proposed system for MI classification

3.1 Dataset

Electrocardiogram data were sourced from the Physikalisch Technische Bundesanstalt (PTB-ECG) database. The dataset includes between one to five recordings per subject, with each record containing 15 leads-12 standard ECG leads and three Frank leads. The number of recordings per subject varies. The signals, sampled at a rate of 1000 Hz with a resolution of 0.5µV, have different durations depending on the individual. Tables 2 and 3 provide a detailed summary of the PTB dataset [25].

Table 2. Summary of PTB dataset

Class	Number of Subjects	Number of Records	Number of 12-Lead Records
Healthy control (HC)	52	80	6945
Myocardial infarction (MI)	113	312	17212
Total	165	392	24157

Table 3. Types of MI

Class	Number of Subjects	Number of Records	Number of 12-Lead Records
Anterior MI (AMI)	17	47	2287
Inferior MI (IMI)	30	89	4452
anteroseptal MI (ASMI)	27	77	4312
Inferolateral MI (ILMI)	23	56	3586
Anterolateral MI (ALMI)	16	43	2575
Total	113	312	17212

3.2 Preprocessing

3.2.1 Signal denoising using EMD-FWPSO

EMD, or Empirical Mode Decomposition, is an adaptive signal-analysis technique developed by Huang et al. [26]. Unlike traditional signal-analysis methods, they do not rely on predefined basis functions. Instead, EMD divides the original signal into sub-signals of varying frequencies by analyzing its trends over characteristic timescales. This approach is adaptable and can be used for various signal analysis applications. The EMD process begins with smoothing the signal, which is then broken down into trends at various timescales. The resulting sequences, which correspond to these different time scales, are known as intrinsic mode functions (IMF).

Empirical Mode Decomposition (EMD) is a signal-processing technique that decomposes a complex signal into a finite set of Intrinsic Mode Functions (IMFs). Each IMF corresponds to an oscillatory mode within the signal arranged from high to low frequencies. This technique is especially useful for analyzing nonstationary and nonlinear signals, such as those found in heart disease datasets, by breaking them down into more manageable components. The FWPSO is an optimization technique that combines PSO and fuzzy logic. PSO is a stochastic optimization algorithm that mimics the social behavior of bird flocks and fish schools. It iteratively refines candidate solutions (particles) towards the optimal solution, considering their historical best performance as well as the best solutions identified by nearby particles. FWPSO improves this approach by incorporating fuzzy logic to address uncertainties and ambiguities in data or optimization parameters, thereby increasing the robustness and adaptability of the optimization process.

EMD-FWPSO employs EMD to decompose noisy heart signals into IMFs, effectively isolating noise and streamlining the data. Subsequently, FWPSO is used to automatically identify the optimal IMFs or establish the best parameters for denoising and feature extraction, ensuring that only the pertinent components of the signal are preserved for further analysis. In predicting heart disease, selecting the correct features (such as shape parameters) from the signal is vital for achieving an accurate classification or prediction. The EMD-FWPSO assists in identifying and selecting these shape parameters by optimizing their weights or contributions based on their relevance in differentiating between healthy and diseased states.

The signal being entered was used as the starting point for the signal-noise removal process. EMD is a method used to deconstruct non-linear and non-stationary time series into a group of IMFs and a residue. This method is adaptable. The IMF in EMD is designed to meet two requirements in the EMD algorithm [27, 28]: (a) for the entire period, the number of zero crossings and greater levels varies by no more than one; and (b) at any moment.

(1) Find all the local extremes of the ECG signal that is currently being examined, and then use a cubic spline approximation to link the local maximum and minimum values to build the upper and lower enclosures of the signal.

(2) Calculate the mean m_{11} as the difference between the ECG signal $x(t)$ and the upper and lower envelopes, and label this difference as the upper envelope $m_{11}(t)$ as new series $h_{11}(t)$. An equation may be used to explain it (1):

$$x(t) - m_{11}(t) = h_{11}(t) \tag{1}$$

If $h_{11}(t)$ meets the two requirements, then you should consider using it as the initial IMF. If not, you should take $h_{11}(t)$ since the initial signal and the procedures described previously are performed repeatedly until the $h_{1k}(t)$ is an IMF and set the $h_{1k}(t)$ as $c_1(t)$. An equation may be used to explain it (2):

$$c_1(t) = h_{1k}(t) \tag{2}$$

In most cases, the Standard Deviation (SD) is used to analyze repetitiveness. When the Standard Deviation (SD) number is lower than a predetermined threshold, typically in the range of 0.2 and 0.3, the process of repeatedly subtracting will end. It is characterized by an Eq. (3):

$$SD = \sum_{t=0}^{T} \left(\frac{\left| h_{1(k-1)}(t) - h_{1k}(t) \right|^2}{\left(h_{1(k-1)}(t) \right)^2} \right) \tag{3}$$

(3) The remaining substance following the separation $c_1(t)x(t)$ is used in the equation that is derived from it (4):

$$x(t) - c_1(t) = r_1(t) \tag{4}$$

(4) Treat the residual $r_1(t)$ as the primary ECG signal, and further iterations of the aforementioned procedure, which will result in the acquisition of additional IMF $sc_i(t), i = 2, \ldots, n$. When the residual is reached, the EMD decomposition will be finished $r_n(t)$ transforms into a function that is monotone. The first ECG signal ever recorded $x(t)$ may be ultimately articulated in the form of an Eq. (5):

$$x(t) = \sum_{i=1}^{N} c_i(t) + r_n(t) \tag{5}$$

Therefore, the original ECG signal is broken down into N different intrinsic magnetic fields as well as a residual $r_n(t)$. By virtue of the repetitive filtration process, the envelope error propagates throughout the local mean and the entire signal, leading to inaccurate and inaccurate deconstruction.

The cubic spline lacks sufficient flexibility when fitting the local extreme values, which is the cause of overshoot and undershoot issues that often arise in the cubic spline. When up-sampling the maxima and minima envelopes during the EMD filtering process, cubic Hermit interpolation is often employed in lieu of cubic splines because it is just first-order smoothness, whereas cubic spline interpolation is of second-order smoothness. The method for cubic Hermit approximation was discovered to sometimes be overly flexible, and this might even result in blatant break points.

The rational Hermit interpolation features a shape determining parameter in contrast to the conventional cubic Hermit interpolation λ. Due to the parameter λ, by altering the parameter's value, it is possible to modify the way the rational Hermite constructs its spline curves λ. As a result, rational Hermit interpolation may be seen as an advancement over cubic Hermit interpolation, and its formulation of the basis function is shown below.

Given a series of discrete data $(x_i, y_i, d_i)(i = 1, 2, \ldots, N)$, the y_i is the time-dependent local maximum and minimumx_i and the d_i wherever possible, is the first iteration x_i ($d_i = dy(t)/dx(t)$). The goal was to interpolate the segments by fitting the two spots. Each of these may be used to generate the reasonable Hermite approximation $[x_k, x_{k+1}]$ ($k = 0, 1, \ldots, N-1$) by Eq. (6):

$$\begin{aligned} s_k(x) = F_i(t)y_i + F_{i+1}(t)y_{i+1} + G_i(t)h_i d_i \\ + G_{(i+1)} h_i d_{i+1} \end{aligned} \tag{6}$$

where, $h_i = x_{i+1} - x_i, t = \frac{(x - x_i)}{h_i}, \lambda$ is the parameter that determines the form that the spline will take. $F_i(t), F_{i+1}(t), G_i(t)$ and $G_{i+1}(t)$ consist of the fundamental operations of the logical Hermite interpolation. In order to show how well the constant variable works λ, a portion of the synthetic ECG signal is subjected to the rational Hermite extrapolation. There is a parameter in the rational Hermite approximation equation λ that allows filtering process users to choose the interpolation's form. Figure 2 illustrates the parameter-selection processes.

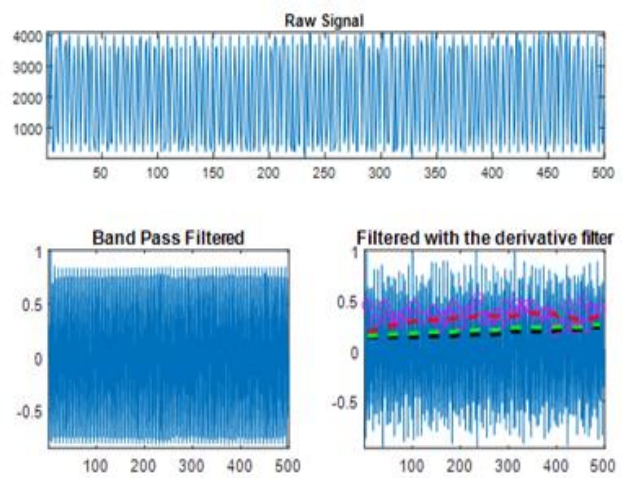

Figure 2. Input signal process

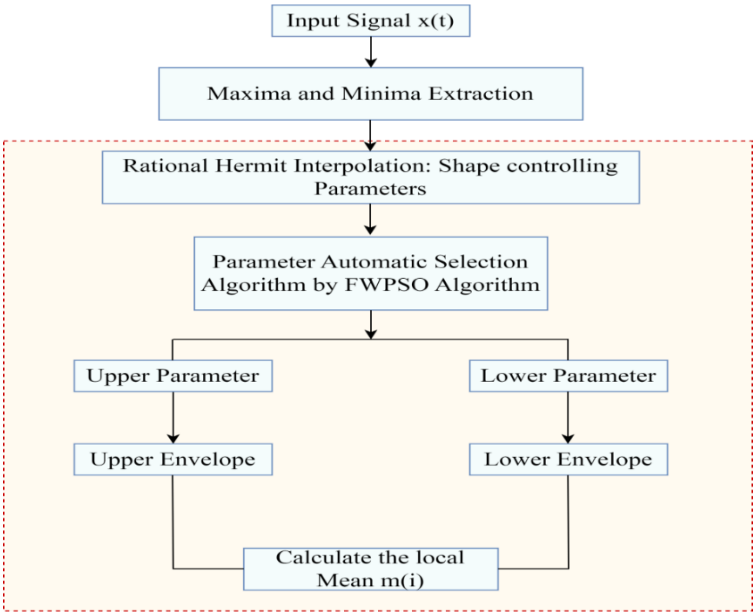

Figure 3. Flow chart of the shape parameter selection procedure with FWPSO algorithm

The upper and lower envelopes' parameters should be independently and labeled as because the waveform and fluctuation trend of the maximum and minimum could be significantly distinct λ_i and λ_j , respectively [29]. It is necessary for the parameter in the sifting process to be adjustable, because the waveform and fluctuating trend of the maxima and minima of the newly created time series. Consequently, the parameter of the logical Hermit is self-adaptively chosen for each sifting phase. In this work, parameter determinant criteria are established and considered as the fitness function to achieve the shape-regulating parameter automated selection using the FWPSO algorithm in each sifting process. The implementation criteria are a linear combination of the relative skewness of the estimated local mean and two indices, the first of which is the minimum range between the midpoint and local mean. The following is an expression for the shape-regulating parameter determinant criteria: Figure 3 shows the flowchart of the selection procedure with the FWPSO algorithm.

In PSO, the search space is scanned by a swarm of Np particles to determine the best solution [30]. The velocity and efficiency ratings are shared by all components. Depending on its own prior best placement and the prior best position of the swarm, each particle (i.e., a possible solution) advances in the search space at a certain speed. To obtain a better search region, the particles fly across the D-dimensional problem space throughout the search process. Two characteristics, namely the particle's present location ($X_{i,k}$) and velocity ($V_{i,k}$) on the search space, define particle I (I=1, 2,...,Np) [31]. The iteration counter may be found at the index k. The following relations determine how the particles in the initial population (k=0) move and place themselves first:

$$X_{i,0}^{j}=X_{Min}+\text{Random }(X_{Max}\text{-}X_{Min}) \tag{7}$$

$$V_{i,0}^{j}=V_{Min}+\text{Random }(V_{Max}\text{-}V_{Min}) \tag{8}$$

where, $X_{i,0}^{j}$ and $V_{i,0}^{j}$ are, in relation to the jth (j=1,2,...,D) dimension, the ith (i=1,2,....Np) particle's location and velocity values, respectively. X_{Min}, X_{Max}, V_{Min} and V_{Max} are the user-defined boundaries, and Random is an evenly distributed random integer generated in (0,1). The following equations update the location and speed of each particle for the subsequent populations (k>0) for i=1, i=2, i=3, i=4,5, i=6, and i=Np:

$$V_{i,k+1}=c_1 r_1(X_{i,k}^{pbest}\text{-}X_{i,k})+c_2 r_2(X_{i,k}^{gbest}\text{-}X_{i,k})+W_k V_{i,k} \tag{9}$$

$$X_{i,k+1}=X_{i,k}+V_{i,k+1} \tag{10}$$

where, $X_{i,k}$ is the situation of the ith particle at the kth iteration, $X_{i,k}^{pbest}$ is the role of the ith particle at the finest prior installment, $V_{i,k}$ is the velocity, c_1 and c_2 are referred to as perceptual and social correlations, r_1 and r_2 are unified random numbers in (0,1), and $X_{i,k}^{gbest}$ is the keep in mind that c_1 and c_2 are the positive constants that, correspondingly, indicate the attraction toward $X_{i,k}^{pbest}$, and $X_{i,k}^{gbest}$ [32]. W_k is the inertial weight that influences the new velocity by acting on the previous velocity.

The linear decreasing approach of fuzzy inertia weighting, in which W_k is updated using the following formula, is one of the most often used techniques:

$$W_i=W_{Max}\text{-}\frac{W_{Max}-W_{Min}}{Iter_{Max}}\times \text{k} \tag{11}$$

where, $Iter_{Max}$ is the maximum number of iterations and W_{Max} and W_{Min} are the weighting coefficient's starting and ultimate levels, correspondingly. The fundamental PSO structure is as follows:

Step 1: Create the particle's starting population location and speed using Eqs. (7) and (8).

Step 2: Utilize relation (9) and update the location and speed of each particle (11).

Step 3: Calculate the relevant fitness values in accordance with the fitness function of the optimization problem after mapping the particle location to the solution space.

Step 4: Update $X_{i,k}^{pbest}$ and $X_{i,k}^{gbest}$.

Step 5: Proceed to Step 2 if the requirements for halting are not satisfied; otherwise, terminate the algorithm.

The following is an explanation of the proposed FWPSO approach:

1) Perform the calculations necessary to determine the local maxima and minima of the IMF.
2) When compared with the adaptable thresholds, the actual numbers of the local maximum and minimum were examined by λ distinct determinations made using the FWPSO algorithm. Produce a partially analyzed IMF by setting the maxima with values lower than the threshold to zero.
3) Perform the calculations necessary to determine all the local maxima and minima of the IMF that were obtained in Step 2.
4) Step 3 involves performing a comparison between the actual numbers of the local maximum and minimum using the same threshold λ, zero out the extremes whose absolute values are lower than the threshold, and obtaining another IMF that has been partially analyzed.
5) Repeat Steps 3 and 4 as many times as necessary until there are no more local maxima and minima that need to be reset to zero.

The proposed approach can save all QRS information. This is accomplished by continually filtering peaks that are lower than the threshold. The Signal-to-Noise Ratio (SNR) is a quantitative evaluation of the performance of the approach. The SNR is the ratio of the amount of usable energy to the amount of noise energy. The equation below describes the definition of signal-to-noise ratio (12):

$$SNR = 10\,log\left(\frac{\sum_{n=1}^{N} s^2(n)}{\sum_{n=1}^{N} n^2(n)}\right) \tag{12}$$

where, $s(n)$ denotes the signal that existed before the introduction of any noise and $n(n)$ refers to the noise that has been incorporated into the signal. Their connections are represented by the equation in the following phrase (13):

$$x(n) = s(n) + n(n) \tag{13}$$

where, $x(n)$ represents the erratic signal. The effectiveness of the denoising algorithms was evaluated by examining the increase in the SNR. This equation describes how the SNR improvement is defined (14):

$$SNR_{imp} = SNR_{denoised} - SNR_{original} \tag{14}$$

A metric for assessing the efficiency considering the energy perspective is the SNR increase. The EMD signal is shown in Figure 4.

3.3 Segmentation

The three components of the heartbeat segmentation process are the detection of P and T waves and the QRS complex.

QRS complex detection: The Pan Tompkins approach identifies the QRS complex on denoised ECG data. The method can be broken down into four steps: derivation, quadratic distinctions, shifting integral, and threshold operations.

Finding a steep slope is one of the steps in the separation process, which is utilized to isolate the QRS complex from other electrocardiogram waveforms. Subsequently, point-to-point squaring of the slope is performed, which is an essential step because it highlights the higher values that mostly arise as a result of the QRS complex. Subsequently, moving-window integration will disclose other information, including the QRS onset, offset, and breadth. Additionally, amplitude thresholds were used to locate the R peaks.

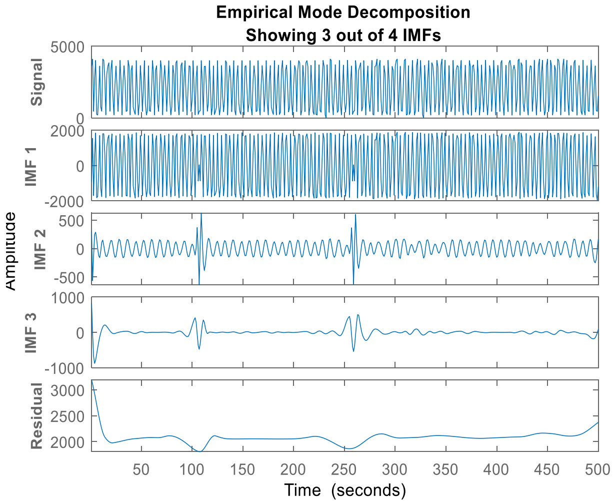

Figure 4. Empirical mode decomposition

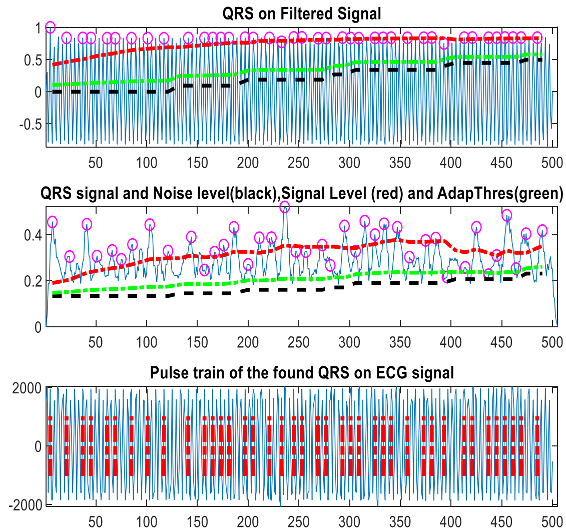

Figure 5. QRS signal

P-and T Waves delineation: Following the identification of the QRS complex, the QRS complex serves as a guide for establishing the boundaries of two search windows that are utilized to simultaneously detect P- and T-waves. The average integral nucleus was located at the P-wave peak. The local minimum and maximum were compared to the corresponding thresholds in the search window, and the T-waves were then calculated [33]. Figure 5 shows the QRS signal.

3.4 Feature extraction

The extracted ECG segments were analyzed using PCA. PCA is to isolate unimportant factors from a large set of important elements. The retrieved ECG segment was subjected to PCA, and the first five columns of the Y variables were considered the five characteristics for further categorization [34].

Reducing the ECG dataset dimensionality with PCA improved the performance of the CKWCNN classifier. PCA effectively reduces noise and emphasizes the most informative features by converting the original high-dimensional data into lower-dimensional space. This results in enhanced computational efficiency and faster training times, while preserving the key characteristics of the ECG signals. Additionally, morphological features offer valuable insights into the structural aspects of ECG signals, including the shapes, peaks, and intervals that are indicative of myocardial infarction. Incorporating these features enables the CKWCNN classifier to detect subtle patterns in the data that are crucial for an accurate classification. This added layer of information strengthens the robustness of the model and enhances its overall accuracy in identifying myocardial infarction. The combination of PCA and morphological features created a more effective feature set, which significantly improved the classification accuracy of the CKWCNN. By integrating these techniques, the model achieved better performance metrics than when using raw ECG data alone, resulting in improved detection rates and fewer false positives. When relying solely on raw ECG data, the model may find it challenging to identify relevant patterns owing to the high dimensionality and noise. In contrast, the integration of PCA and morphological features facilitates a more targeted analysis, leading to increased classification accuracy and a lower false-positive rate.

The issue of low-dimensional feature modeling is outlined below.

Let X=$(x_1, x_2, \ldots, x_n)$ each x_i is an ECG feature vector of size n, and represents the *n* by N data matrix.

3.4.1 Computing the scatter matrix

The scatter matrix is computed as follows:

$$S=\sum_{k=1}^{n}(x_k - m)(x_k - m)^T \tag{15}$$

where, *m* represents the mean vector.

The recommended approach calculates the mean values for increasing the dimension reduction probability.

$$m=np \tag{16}$$

where, the beats observed are indicated by the number *n*. *p* is the probability of success.

3.4.2 Computing eigenvectors and corresponding eigenvalues

When we extracted the component using covariance, the eigenvectors were multiplied by it. Let us verify that the equation is satisfied and that the eigenvector-eigenvalue computation is accurate.

$$\sum v=\boldsymbol{\lambda}\mathrm{v} \tag{17}$$

where, $\sum -covariancematrix$, *v*-Eigen vector and $\boldsymbol{\lambda}$-Eigen value.

It is recommended to eliminate the eigenvalues with the lowest eigenvalues because they reveal the least information regarding the data distribution [35]. The usual method is to choose the top k eigenvectors by ranking the eigenvectors according to their associated eigenvalues from highest to lowest. Creating our dk-dimensional eigenvector matrix in this case requires merging the two eigenvectors with the highest eigenvalues W^T.

The samples are transformed onto the new subspace using the equation in the last step using the 23-dimensional matrix W that the system just generated y=W^T×x. Following are the steps:

1) Consider the entire collection of information composed of examples with d dimensions.
2) Calculate the mean vector across all the dimensions.
3) The overall correlation matrix of the information set is created.
4) Compute eigenvectors $(e_1, e_2, \ldots, e_d)$ eigenvalues that relate to the various variables $(\boldsymbol{\lambda}_1, \lambda_2, \ldots, \lambda_d)$.
5) To create a matrix with dimensions d×k, the eigenvectors are arranged in descending order of their eigenvalues, and then choose the k eigenvectors that have the highest eigenvalues W.
6) To convert the samples into a new subspace, the dk eigenvector matrix may be used. The mathematical equation may be used to provide a concise summary of this: y=W^T×x (where x is ad×1-One sample is represented by a one-dimensional vector, and the converted k-by-one-dimensional sample in the new subspace is represented by y.

3.5 Classification

3.5.1 Convolution weight based CNN (CWCNN) classifier

This research aimed to categorize myocardial infarction via a Convolution Kernel Weight-Based Convolutional Neural Network (CWCNN). This network primarily comprises convolutional, subsampling or pooling, and fully linked layers [36]. This network architecture has an input layer that receives the selected characteristics, an output layer that produces the trained results, and several intermediary layers referred to as hidden layers as shown in Figure 6.

Convolution Layer

A convolutional neural network (CNN) commences with a convolutional layer as its initial component. This layer executes convolution by utilizing a kernel (or filter) for the input characteristics.

To provide the output [37], each characteristic of the input matrix underwent convolution with the kernel. The output is represented as n and is obtained by convolutionating the input and the kernel. The kernel of a convolution matrix is commonly termed a filter, and the output generated from applying this filter to the input is referred to as a feature map, which possesses dimensions i*i.

In the subsequent convolutional layers of the network, the inputs and outputs consist of feature vectors. Each convolutional layer utilized a collection of n filters. The input undergoes convolution with these filters and the depth of the resultant feature maps (n) correlates with the number of filters employed. Each filter map denotes a distinct feature that is derived from a specific input area.

The output of the lth convolution layer is denoted by the symbol$C_i^{(l)}$ is derived as follows:

$$C_i^{(l)}=B_i^{(l)} + \sum_{j=1}^{a_i^{(l-1)}} K_{i,j}^{(l-1)} * C_j^{(l)} \tag{18}$$

where, $B_i^{(l)}$ represents the bias matrix $K_{i,j}^{(l-1)}$ through a convolution filter from the preceding layer (l - 1) incorporating the ith feature map alongside the others. The results of the work $C_i^{(l)}$ constitutes the feature maps of the layer in question. In (18), the intial layer of CNN network $C_i^{(l-1)}$ is a place for input, which is $C_i^{(0)} = X_i$.

The kernel then generates a feature map. After applying the convolution layer:

$$Y_i^{(l)} = Y(C_i^{(l)}) \tag{19}$$

where, $Y_i^{(l)}$ represents the activating factor and $C_i^{(l)}$ denotes the data that is inputted into it.

The three most commonly adopted activation functions are sigmoid, tanh, and rectified linear units (ReLUs). The research occasionally refers to weighted ReLUs is $\mathrm{Y}_\mathrm{i}^{(\mathrm{l})} = \mathrm{w}.\max(0, \mathrm{Y}_\mathrm{i}^{(\mathrm{l})})$. The activation function is frequently used in deep learning models because of its efficacy in mitigating the detrimental impacts of interactions and nonlinearity and is essential for improving model performance. In this case, we employ a Rectified Linear Unit (ReLU) activation function [38]. For negative inputs, the ReLU outputs 0 and maintains the input value for positive inputs. This function is helpful because it accelerates learning by fixing the vanishing gradient problem. In the saturation zones, the gradient becomes much smaller, which means that the training weights do not change significantly.

We integrated the feature weights to enhance the performance. We calculate the convolution kernel weights based on the significance of the features instead of assigning them randomly. The primary benefit of using these convolution weights is that they reduce classification mistakes by considering the significance of the features derived from the data. Thus, the kernel recognizes the features to obtain weights (Figure 7).

Pooling Layer

Following the convolutional layer, the subsampling layer aims to reduce the spatial dimensions of the map features from the previous convolutional layer [39]. We accomplished this reduction by partitioning the feature maps into 2×2 blocks and calculating the average value for each block. The subsampling layer maintains the relative information among the features instead of their precise relationships. Incorporating a subsampling layer improves the resilience of the convolutional layer to translation and rotation in the input data.

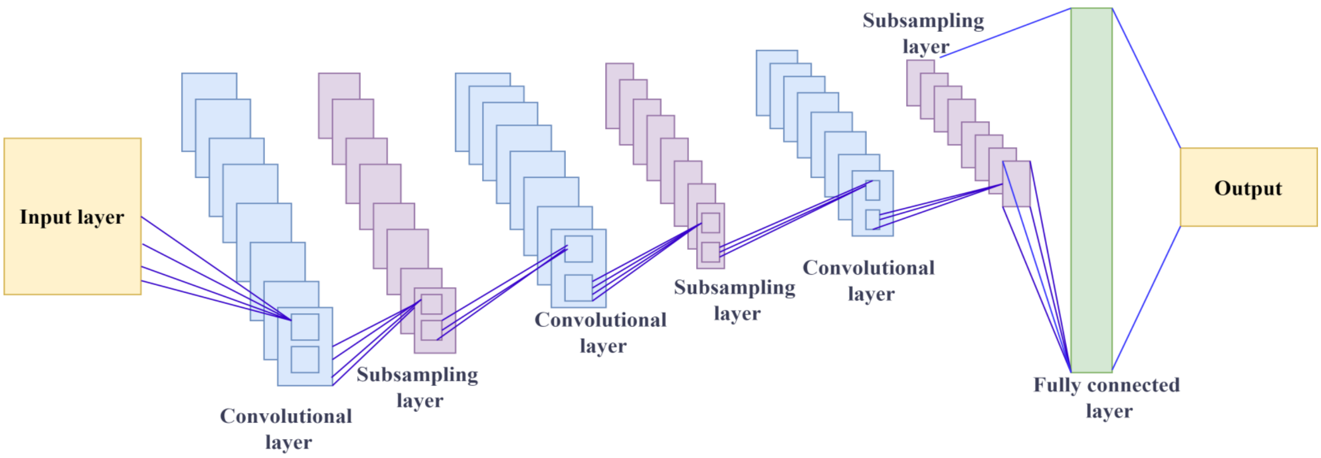

Figure 6. Convolutional neural network (CNN)

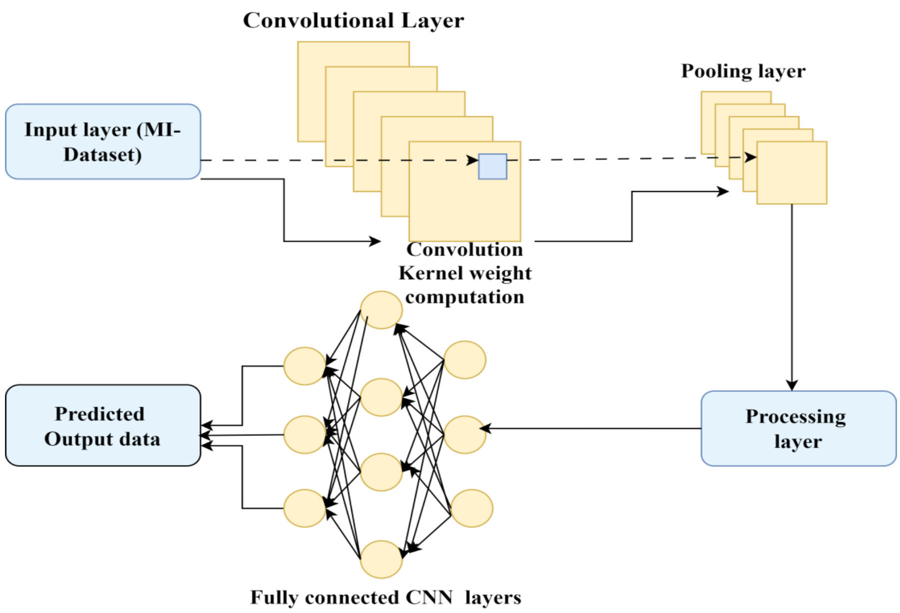

Figure 7. Convolution Kernel Weight Based CNN (CKWCNN) classifier

Fully Connected Layer

The output layer uses softmax activation:

$$Y_i^{(l)} = f(z_i^{(l)}), \tag{20}$$

where, $z_i^{(l)} = \sum_{i=1}^{m_i^{(l-1)}} w_{i,j}^{(l)} y_i^{(l-1)}$.

where, $w_{i,j}^{(l)}$ denotes the completely linked layer must alter weight values to reflect each class, and f represents the transfer function, which denotes nonlinearity.

Pseudo code algorithm: Convolutional Kernel Weight based CNN classifier

Input: Selected features x_1, x2, x3....x_n, target label T (y_1....y_T), Number of convolutional masks size, Number of epochs for Forward Propagation and Backward Propagation

Output: Predicted Labels

Steps:

1: Start

2: sf(Xi) ← Get selected features

3: Normalize the feature data

4: regularization feature data

5: Repeat every epoch

6: Perform forward propagation until epochs

7: cd ← Convolution (sf sf(Xi))

8: mp ← pooling (cd)

9: fc ← fully _connected (mp)

10: calculate weight w_i using Convolution kernel till convergence completed

11: class label ← Soft_max (fc)

12: Do Backward Propagation till R

13: Conduct backward propagation

14: Obtain the output predicted labels Yi

15: End.

4. RESULTS AND DISCUSSION

In this section, the outcomes of the suggested approach and previously suggested methods for MI identification are compared. The proposed method was discussed and implemented using MATLAB. This innovative effort demonstrates encouraging outcomes in the medical field, which inspires confidence that such patients may be accurately and quickly identified.

We used the PTB dataset to identify myocardial infarctions and test how well the proposed CKWCNN algorithm worked in both inter-patient and intra-patient settings. The evaluation focused on measures such as accuracy, sensitivity, specificity, precision, and F-measure. We utilized a 5-fold cross-validation method to mitigate the impact of initialization on networks.

The beats were randomly allocated into five approximately equal pieces using the intra-patient method. We employed three segments for model training during each cycle: one segment served as the validation set for parameter optimization, while the remaining segment served as the testing set to evaluate the final performance. For training, validation, and testing, the inter-patient method randomly assigned patients in a 3:1:1 ratio, designating the respective beats for each set.

We averaged performance indicators, such as accuracy, sensitivity, specificity, precision, and F-measure, after concluding all five iterations to provide a comprehensive evaluation of the model's efficacy. Employing many methods guarantees that the evaluation accurately represents the model's performance across various data distributions, thus enhancing the dependability of the results. The 5-fold cross-validation facilitates the generalization of the model to novel data, thereby diminishing the probability of overfitting to a particular training set. This approach ensures a comprehensive assessment of the performance of the model by training it on diverse data segments and undergoing distinct testing with each iteration.

This section discusses the performance of MI detection and localization based on a 5-fold cross-validation. Mainly, 24,157 data points containing HC with different MI were separated into five equal sections, with the same number in each of the two MI detection categories and the same number in each of the six MI localization categories. During the training phase, 19,326 HC and MI records were used. Instead, 4,831 records were used during the testing stage. Thus, all 24157 records were used based on cross-validation.

Precision is defined as the ratio of accurately identified positive discoveries to total predicted positive results.

$$Precision = \mathrm{TP} / \mathrm{TP} + \mathrm{FP} \tag{21}$$

Recall is defined as the ratio of accurately identified positive data to total data within an appropriate classification.

$$Recall == \mathrm{TP} / \mathrm{TP} + \mathrm{FN} \tag{22}$$

The F1 score is the weighted average of the precision and recall. Thus, they may produce false positives and negatives.

$$\text{F1 Score=} \quad 2 *(\text{ Recall * Precision }) /(\text{ Recall + Precision }) \tag{23}$$

Specificity measures the percentage of correct negatives observed.

$$Specificity = \mathrm{N} / \mathrm{FP} + \mathrm{TN} \tag{24}$$

Accuracy is the overall accuracy of the model, and is determined by dividing the total number of real classification parameters by the total number of classification parameters. The accuracy is calculated as

$$Accuracy = \mathrm{TP} + \mathrm{TN} / (\mathrm{TP} + \mathrm{FP} + \mathrm{TN} + \mathrm{FN}) \tag{25}$$

The error rate calculation is performed as follows,

$$\text{Error=100-Accuracy} \tag{26}$$

The terms "True Positive," "True Negative," "False Positive" and "False Negative," are abbreviated as "TP," "TN," "FP," and "FN," respectively.

4.1 Performance evaluation using the intra-patient approach

Table 4 and Figure 8 show the overall performance based on MI detection using the intra-patient scheme in conjunction with the CKWCNN model. Table 4 shows that the overall performance, which includes accuracy, recall, specificity, precision, and F1, was 99.9%, 99.99%, 99.73%, 99.87%, and

99.88%, respectively. Only 0.19% of the ECG recordings were misidentified in the fifth run of the experiment, thereby demonstrating the superiority of the proposed approach. Figure 9 shows that only two MI and 11 HC records were misclassified. In addition, 17,210 IM data points were successfully detected out of 17,212 records, indicating a very low false-negative rate.

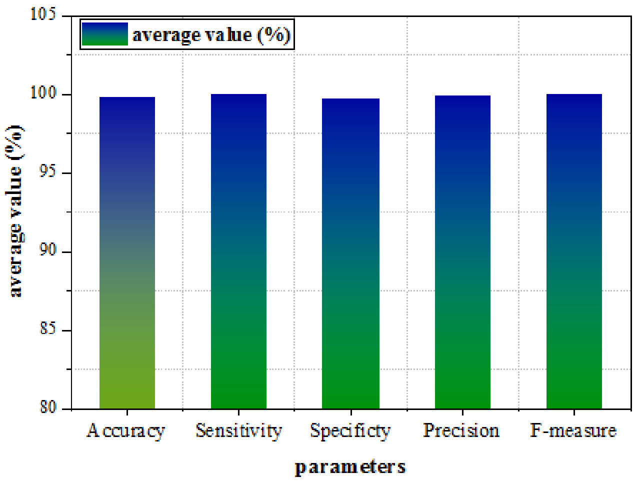

Figure 8. Comparison outcomes for MI detection using the intra-patient approach

However, myocardial infarction localization is more complicated than myocardial infarction detection, which is characterized by dynamic changes in different ECG leads. The CKWCNN model correctly identified data in the ASMI, AMI, ALMI, ILMI, IML, and HC categories, as shown in Table 5, achieving a superior average performance of 5folds. The precision, sensitivity, specificity, and F1 values were 99.82%, 99.73%, 99.82%, and 99.78%, respectively.

Figure 10 shows the confusion matrix and MI localization performance of the intra-patient 5-fold cross-validation scheme. It is easy to see that 12 AMI data and 12 ALMI data points are considered ASMI. In fact, all the above data are from previous MI, making it difficult to differentiate between these groups. As shown in Figure 11, almost no IMI data were witnessed as HC or AMI data. In contrast to the intra-patient experiments mentioned earlier, the inter-patient scheme has considerable clinical importance for demonstrating the model's generalization capabilities. For the PTB database, the training phase involved 55 healthy controls (HC) and 209 myocardial infarction (MI) patients, while the test phase included the remaining 25HC and 103 MI patients. A total of 4,740HC and 10,721 MI 12-lead ECG recordings were utilized for training, and after preprocessing, 2,205HC and 6,491 MI recordings were used to assess the protocol performance across patients.

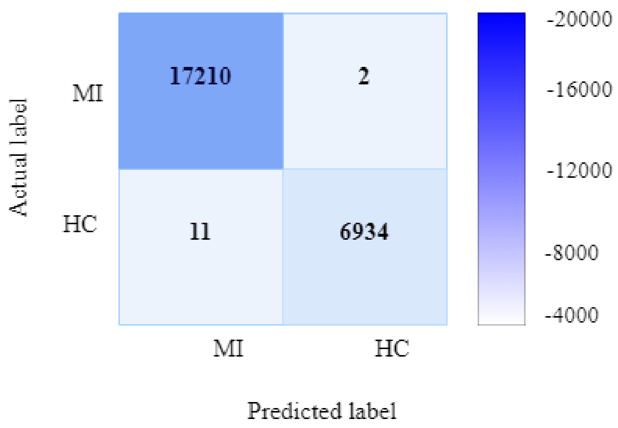

Figure 9. Confusion matrix and performance for MI detection using the intra-patient approach

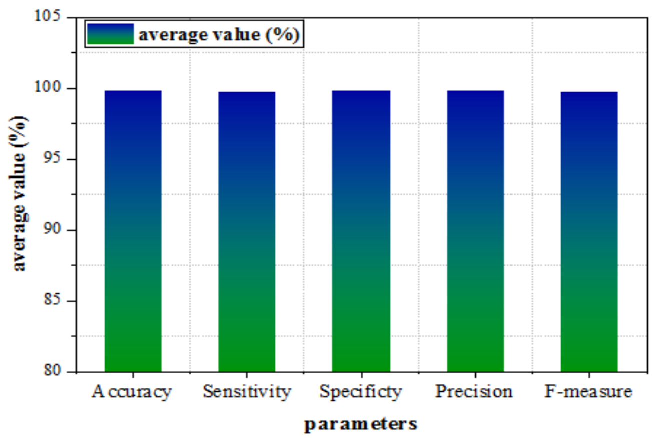

Figure 10. Comparison outcomes of MI localization using the intra-patient approach

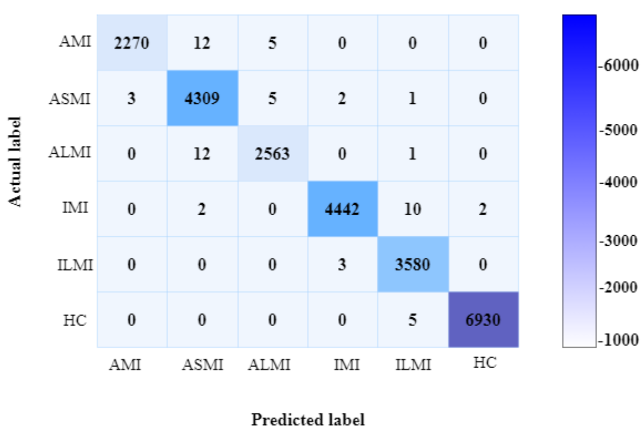

Figure 11. Confusion matrix and performance for MI localization using the intra-patient approach

Table 4. 5-fold cross-validation outcomes for MI detection using the intra-patient approach

Fold	Accuracy (%)	Sensitivity (%)	Specificity (%)	Precision (%)	F-Measure (%)
1	99.83	99.97	100	100	99.85
2	99.77	100	99.41	99.71	99.81
3	99.98	100	100	100	100
4	99.99	100	100	100	100
5	99.72	100	99.27	99.65	99.78
Average	**99.9**	**99.99**	**99.73**	**99.87**	**99.88**

Table 5. 5-fold cross-validation outcomes for MI localization using the intra-patient approach

Fold	Accuracy (%)	Sensitivity (%)	Specificity (%)	Precision (%)	F-Measure (%)
1	99.72	99.58	99.71	99.67	99.62
2	99.84	99.79	99.84	99.79	99.79
3	99.92	99.89	99.92	99.89	99.89
4	99.92	99.86	99.92	99.92	99.89
5	99.74	99.57	99.73	99.63	99.65
Average	**99.82**	**99.73**	**99.82**	**99.78**	**99.76**

4.2 Performance evaluation using the inter-patient approach

Combining the results in Table 6 and Figure 12, it is clear that our algorithm achieves good overall performance based on MI detection using the interpatient approach in conjunction with the CKWCNN algorithm. Table 6 shows that the overall performance, which includes the accuracy, recall, specificity, precision, and F1, was 98.74%, 97.91%, 98.75%, 99.57%, and 98.22%, respectively. As shown in Figure 13, only 329 MI and 55 HC records were misclassified.

In addition, 6162 MI data were successfully detected from the 6491 records, indicating a very low false-negative rate. However, myocardial infarction localization is more complicated than myocardial infarction detection, which is characterized by dynamic changes in different ECG leads. Figure 14 indicates that the accuracy and other performance metrics for MI localization are inferior relative to those of all prior tests. The HC class achieved an optimal sensitivity of 96.53%, indicating accurate identification of the majority of HC records.

Table 7 presents a comparison of the classification results. The performance of the precision, recall, and f-measure comparison results of the proposed CKWCNN for MI detection are shown in Figure 15. Therefore, the findings demonstrate that the use of FWPSO for feature selection may be efficient for predicting psychological disorder detection. This is an appealing property because it does not require tuning the overfitting problem in the classifier. The proposed FWPSO is highly effective for solving classification problems. The results show that the proposed method has a recall rate of 89.68%, whereas the state-of-the-art method has a lower recall rate, 66.25% for the SVM method measurement and 67% and 68.54% for the RF and KNN method measurements, respectively.

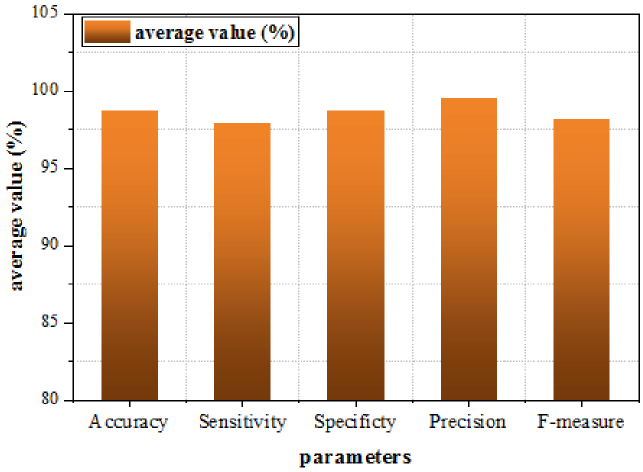

Figure 12. Comparison results of MI detection using inter-patient scheme

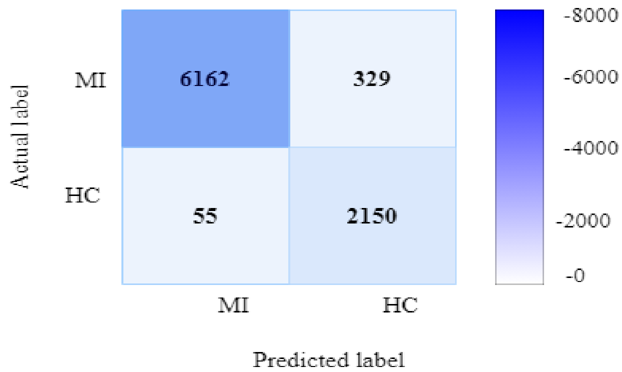

Figure 13. Confusion matrix and performance for MI detection using the inter-patient approach

Table 6. 5-fold cross-validation outcomes for MI detection using the inter-patient approach

Fold	Accuracy (%)	Sensitivity (%)	Specificity (%)	Precision (%)	F-Measure (%)
1	98.72	97.86	98.19	99.05	97.74
2	98.66	97.89	98.30	99.60	97.70
3	98.87	97.90	98.56	99.65	98.12
4	98.88	97.95	99.16	99.77	98.67
5	98.61	97.99	99.54	99.79	98.89
Average	**98.74**	**97.91**	**98.75**	**99.57**	**98.22**

Table 7. Classification results comparison of the proposed CKWCNN classifiers on MI detection

METHODS	METRICS (%)					
	Precision	Recall	F-Measure	Accuracy	Specificity	ERROR
KNN	68.50	70.00	69.24	70.00	73.12	30.00
RF	70.00	69.90	70.00	70.00	78.56	30.00
SVM	75.60	75.10	75.84	75.00	80.78	25.00
BBNN	80.95	89.32	87.00	90.05	92.12	18
CNN	96.00	96.60	96.29	95.00	95.02	12.00
CKWCNN	98.22	99.82	98.38	98.46	98.13	5.00

Table 8. Classification results comparison of the introduced CKWCNN classifiers on MI localization

METHODS	METRICS (%)					
	Precision	Recall	F-Measure	Accuracy	Specificity	ERROR
KNN	57.20	50.00	58.13	65.00	68.23	45.00
RF	60.11	58.81	61.33	71.00	70.45	38.00
SVM	66.71	64.21	64.72	72.19	75.67	29.00
BBNN	70.84	68.43	78.11	80.05	85.23	15
CNN	74.05	70.71	84.18	85.10	90.11	10.00
CKWCNN	90.33	89.93	90.49	89.45	92.24	7.00

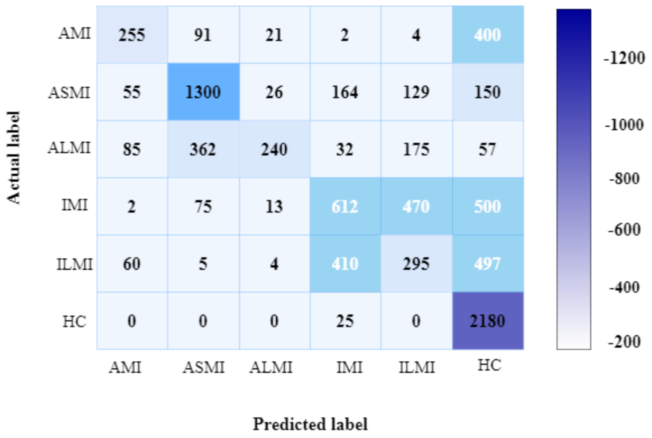

Figure 14. Confusion matrix and performance for MI localization using the inter-patient approach

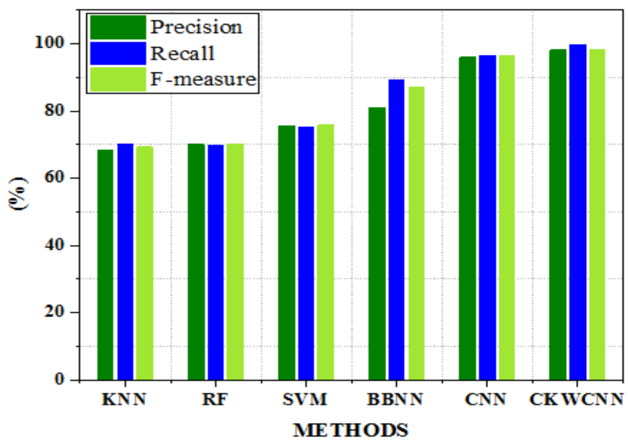

Figure 15. Performance comparison results of the introduced CKWCNN classifier in terms of precision, recall and f-measure on MI detection

Figure 16 illustrates the performance results of the proposed CKWCNN technique. The suggested CKWCNN classifier obtains phenomenal efficiency in terms of the illness detection rates. This can be seen in the graph. The findings of the subjective study, which made use of several machine learning methodologies, and the results of the statistical study, which measured everything in terms of the f-measure in accordance. The accuracy of the proposed CKWCNN was evaluated in comparison to that of conventional categorization algorithms using the MI dataset. The findings indicate that the proposed approach produces a highly specific result of 95%. In contrast, the state-of-the-art method produced poor recall results, such as 80.78% for the SVM method metric and 78.56 and 73.14% for the RF and KNN method parameters, respectively. The proposed CKWCNN-based classifiers provide a lower error rate than the existing classifiers, and Table 8 compares the classification results the performance of the precision, recall, and f-measure comparison results of the proposed CKWCNN for MI localization are shown in Figure 17. Therefore, the findings demonstrate that the use of FWPSO for feature selection may be efficient for predicting psychological disorder detection. This is an appealing property because it does not require tuning the overfitting problem in the classifier. The proposed FWPSO is highly effective for solving classification problems. The results show that the proposed method has a recall rate of 89.93%, whereas the state-of-the-art method has a lower recall rate, that is, 50.00% for the SVM method measurement and 58.81% and 6421% for the RF and KNN method measurements, respectively.

Figure 18 illustrates the performance results of the proposed CKWCNN technique in terms of the accuracy, specificity, and error. The suggested CKWCNN classifier obtains phenomenal efficiency in terms of the illness detection rates, which is significantly better than that of the KNN, RF, SVM, BBNN, and CNN classifiers. This can be seen in the graph. The accuracy of the proposed CKWCNN was evaluated in comparison to that of conventional categorization algorithms using the MI dataset. The findings indicated that the proposed approach produced a highly specific result of 92.24%.

In contrast, the state-of-the-art method produced poor recall results, such as 68.23% for the SVM method metric and 70.45 and 75.67% for the RF and KNN method parameters, respectively. The proposed CKWCNN-based classifiers provide a lower error rate than existing classifiers. Figure 19 shows the proposed confusion matrix and Figure 20 shows the training and validation. Therefore, the performance of the classifications will be greater when compared to other classifications constructed on already developed models and fresh information that is comparable to the entire dataset.

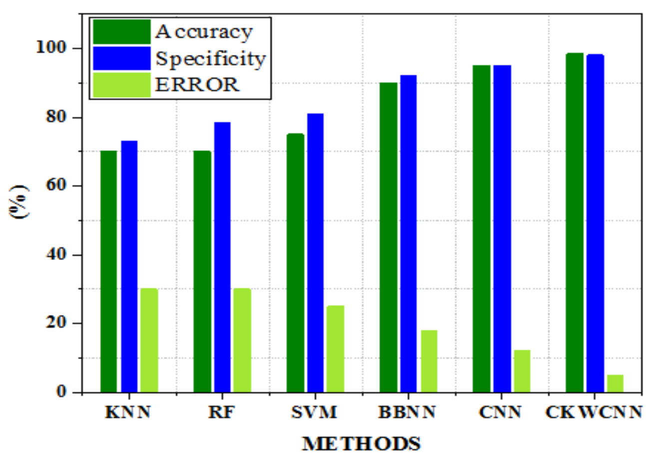

Figure 16. Performance comparison results of the introduced CKWCNN classifier in terms of accuracy, specificity and error on MI detection

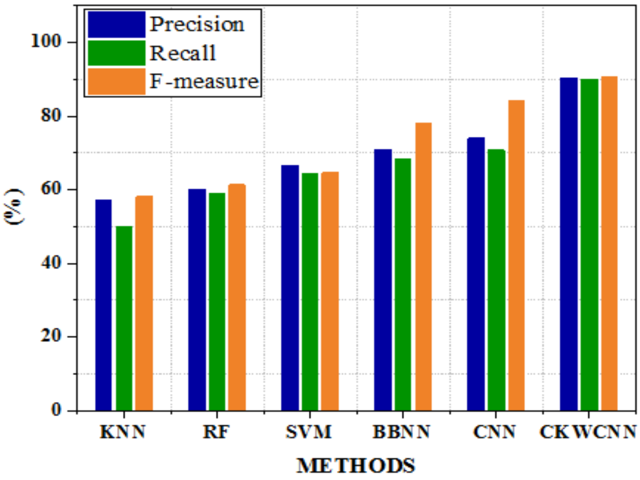

Figure 17. Performance comparison results of the CKWCNN classifier in terms of precision, recall and f-measure on MI localization

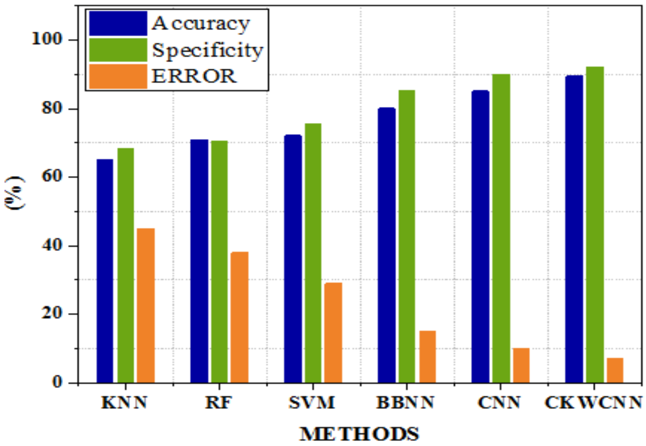

Figure 18. Performance comparison results of the CKWCNN classifier in terms of accuracy, specificity and error on MI localization

```
-------------------------------------------
            Actual Classes
-------------0---------1-----
Predicted|
  Classes|
_________|___________________
       0 |    115.0 |     9.0
       1 |    5.0 |    139.0
-------------------------------------------
-------------------------------------------
            Actual Classes
-----------------------------0---------1-----
True Positive               |   115.00 |   139.00
False Positive              |   9.00 |   5.00
False Negative              |   5.00 |   9.00
True Negative               |   139.00 |   115.00
Precision                   |   0.94 |   0.98
Recall or Sensitivity       |   0.98 |   0.96
Specificity                 |   0.94 |   0.96
-------------------------------------------
```

Figure 19. Confusion matrix of the proposed CKWCNN technique

4.3 Results comparing raw data with proposed PCA

PCA was utilized to decrease the dimensionality of the ECG data, improve computational efficiency, and emphasize important variations within the dataset. Morphological features provide essential insights into the shape and characteristics of ECG signals, which are critical for MI detection. In this section, we will compare the optimal results of the raw data with those obtained using auto-encoder (AE), factor analysis (FA).

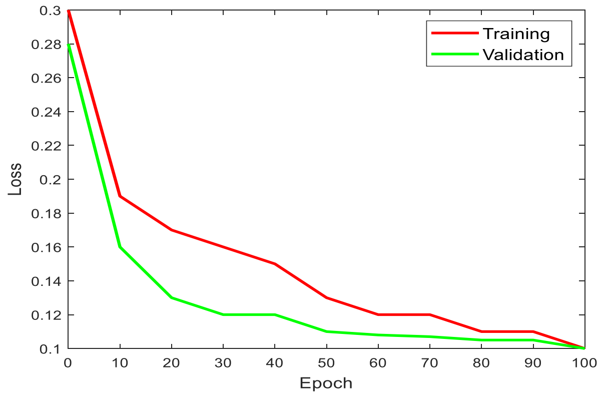

Figure 20. Training and validation of the CKWCNN classifier

Figures 21 and 22 illustrate the performance analysis of both the proposed and existing algorithms for the raw ECG dataset, AE, FA, and PCA-processed datasets using accuracy and F-measure as metrics. The findings indicate that the integration of PCA and morphological features substantially boosts the classification accuracy, with the combined method showing a significant improvement over the use of raw ECG data alone.

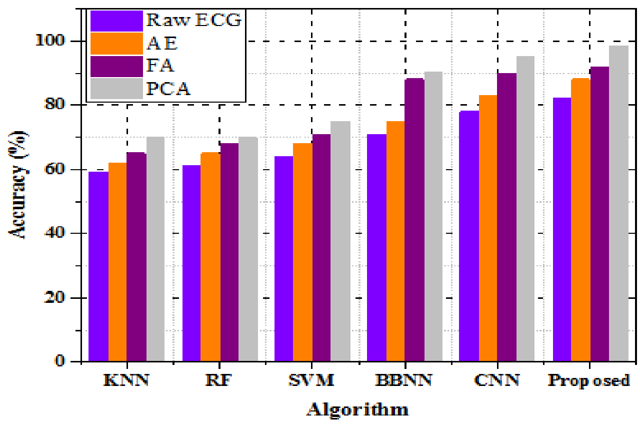

Figure 21. Comparison of results using accuracy

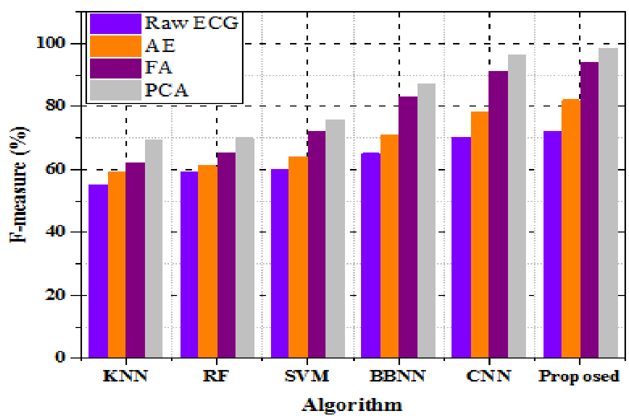

Figure 22. Comparison of results using F1 score

Table 9. State-of-the-art algorithm based ECG MI detection and localization

Reference	Year	Algorithm	MI Detection	MI Localization	Inter-/Intra Patient Analysis
[40]	2018	Google's Inception V3	Accuracy=89.5% F-measure=89.1% Specificity=84.8% Sensitivity=84.3%	-	-
[41]	2018	Multiple-Feature Branch CNN (MFB-CNN)	Intra-: Accuracy=99.9% Specificity=99.9% Sensitivity=99.9% Inter-: Accuracy=98.6% Spec=99.4% Sensitivity=98.7%	Intra-: Accuracy=99.8% Inter-: Accuracy=93.7%	Inter- and intra-patient analysis
[34]	2019	PCANet	Intra-: Accuracy=99.5% Specificity=98.1% Sensitivity=99.8% Inter-: Accuracy=93.2% Specificity=89% Sensitivity=94%	-	Inter- and intra-patient analysis
[42]	2020	CNN	Accuracy=94.8% F-measure=94% Specificity=95.9% Sensitivity=96.4%	-	-
[43]	2021	CNN with fully connected feed forward network	Accuracy=77% Specificity=84% Sensitivity=70%	-	Intra- and inter-patient analysis
[44]	2020	DenseNet	Intra-: Accuracy=99.7% Specificity=99.8% Sensitivity=98.7% Inter-: Accuracy=96.9% Sensitivity=89.2% Specificity=97.8%	-	Intra- and inter-patient analysis
[45]	2021	deep CNN	Specificity=99.7% Accuracy=99.8% Sensitivity=99.9%		-
[46]	2021	ConvNetQuake	Intra-: Accuracy=99.3% Sensitivity=99.4% Specificity=99.5% PPV=99.5% Inter-: Accuracy=97.8%	-	Intra- and inter-patient analysis
[47]	2021	ML-CNN	Accuracy=99.5% Sensitivity=99.7% Specificity=99.4%	PPV=99.3% Sensitivity=99.1% F1-score=99%	-
Proposed		CKWCNN	intra-patient Accuracy=99.9% Specificity=99.73% Sensitivity=99.9% inter-patient Accuracy98.74% Sensitivity=97.91% Specificity=98.75%	intra-patient Accuracy:99.82% Specificity=99.82% Sensitivity=99.73% inter-patient Accuracy=98.65% Specificity=98.56% Sensitivity=98.83%	Intra- and inter-patient analysis

Table 9 depicts the state-of-the-art algorithm-based ECG MI detection and localization. From the table, the proposed method surpasses existing models such as CNN, Deep CNN, Google's Inception V3, ML-CNN, and DenseNet in both intra-patient and inter-patient schemes for myocardial infarction detection and localization. To fully harness CKWCNN's potential for enhancing patient care and outcomes in cardiology, it is crucial to tackle these challenges through thorough validation, regulatory compliance, clinician training, and stakeholder involvement.

4.4 State-of-the-art comparison

The integration of the CKWCNN classifier for MI detection has significant clinical implications, contributing to improvements in the diagnostic accuracy and patient care pathways. CKWCNN's capability of CKWCNN to analyze ECG signals for MI detection can enhance its accuracy beyond traditional methods. By autonomously learning and extracting intricate patterns from ECG data, the CKWCNN may identify subtle changes indicative of MI earlier than conventional techniques. This early detection can facilitate timely intervention, potentially lowering mortality and morbidity rates related to myocardial infarction. Integrating the CKWCNN into clinical workflows can serve as a valuable decision-support tool for healthcare professionals. By offering rapid and objective assessments of myocardial infarction risk through ECG analysis, the CKWCNN can aid clinicians in making timely and informed decisions regarding patient management, including initiating appropriate treatments or referrals to specialized care. The proposed CKWCNN for MI detection has the potential to transform clinical practice by improving diagnostic accuracy, enhancing clinical decision support, and reducing mortality and morbidity rates among patients. However, implementation challenges, such as variations in ECG signal quality, patient demographics, and clinical contexts, can affect CKWCNN's performance and generalizability of CKWCNNs across diverse populations and healthcare settings. To fully harness the CKWCNN's potential for enhancing patient care and outcomes in cardiology, we will address these barriers in the future through comprehensive validation, regulatory compliance, clinician education, and active stakeholder engagement.

5. CONCLUSION

This work concentrates on the early detection of myocardial infarction (MI), which, when performed using the suggested CKWCNN Algorithm, has the potential to save lives worldwide. It is the delayed identification of an illness that is to blame for the decline in the sufferer's quality of life, as well as the value of life of those connected to the afflicted. It is of utmost importance to perform precise and prompt identification. The extraction and selection of features is an important step in the process of constructing a model. This is helpful in eliminating features that provide the least influence. The EMD-FWPSO and PCA solutions suggest this essential goal, each of which achieves global optimization to a commendable degree and represents a fresh method inside this industry. This method has been used to attain an accuracy that is very close to the ideal at every stage of life. The suggested effort will enhance categorization. Finally, the CKWCNN performance was compared to KNN, RF, and SVM in terms of recall, precision, F-measure, and accuracy. This study also reduced the classifier time complexity by employing deep-learning classifiers.

REFERENCES

[1] Banerjee, A., Chen, S., Pasea, L., Lai, A.G., Katsoulis, M., Denaxas, S.,Nafilyan, V., Williams, B., Wong, W.K., Bakhai, A., Khunti, K., Pillay, D.,Noursadeghi, M., Wu, H., Pareek, N., Bromage, D., McDonagh, T.A., Byrne, J., Teo, J.T.H., Shah, A.M., Humberstone, B., Tang, L.V., Shah, A.S.V., Rubboli, A., Guo, Y., Hu, Y., Sudlow, C.L.M., Lip, G.Y.H., Hemingway, H. (2021). Excess deaths in people with cardiovascular diseases during the COVID-19 pandemic. European Journal of Preventive Cardiology, 28(14): 1599-1609. https://doi.org/10.1093/eurjpc/zwaa155

[2] Bansal, M. (2020). Cardiovascular disease and COVID-19. Diabetes & Metabolic Syndrome: Clinical Research & Reviews, 14(3): 247-250. https://doi.org/10.1016/j.dsx.2020.03.013

[3] Jayaraj, J.C., Davatyan, K., Subramanian, S.S., Priya, J. (2019). Epidemiology of myocardial infarction. Myocardial Infarction, 10: 9-17. http://doi.org/10.5772/intechopen.74768

[4] Enas, E.A., Varkey, B., Dharmarajan, T.S., Pare, G., Bahl, V.K. (2019). Lipoprotein (a): An independent, genetic, and causal factor for cardiovascular disease and acute myocardial infarction. Indian Heart Journal, 71(2): 99-112. https://doi.org/10.1016/j.ihj.2019.03.004

[5] Alzahrani, T., Nguyen, T., Ryan, A., Dwairy, A., McCaffrey, J., Yunus, R., Forgione, J., Krepp, J., Nagy, C., Mazhari, R., Reiner, J. (2019). Cardiovascular disease risk factors and myocardial infarction in the transgender population. Circulation: Cardiovascular Quality and Outcomes, 12(4): e005597. https://doi.org/10.1161/CIRCOUTCOMES.119.005597

[6] Murat, F., Yildirim, O., Talo, M., Baloglu, U.B., Demir, Y., Acharya, U.R. (2020). Application of deep learning techniques for heartbeats detection using ECG signals-analysis and review. Computers in Biology and Medicine, 120: 103726. https://doi.org/10.1016/j.compbiomed.2020.103726

[7] Strodthoff, N., Wagner, P., Schaeffter, T., Samek, W. (2020). Deep learning for ECG analysis: Benchmarks and insights from PTB-XL. IEEE Journal of Biomedical and Health Informatics, 25(5): 1519-1528. https://doi.org/10.1109/JBHI.2020.3022989

[8] Teja, K., Tiwari, R., Mohanty, S. (2020). Adaptive denoising of ECG using EMD, EEMD and CEEMDAN signal processing techniques. Journal of Physics: Conference Series, 1706(1): 012077. https://doi.org/10.1088/1742-6596/1706/1/012077

[9] Singhal, A., Singh, P., Fatimah, B., Pachori, R.B. (2020). An efficient removal of power-line interference and baseline wander from ECG signals by employing Fourier decomposition technique. Biomedical Signal Processing and Control, 57: 101741. https://doi.org/10.1016/j.bspc.2019.101741

[10] Sraitih, M., Jabrane, Y., Hajjam El Hassani, A. (2022). A robustness evaluation of machine learning algorithms for ECG myocardial infarction detection. Journal of Clinical Medicine, 11(17): 4935. https://doi.org/10.3390/jcm11174935

[11] Tripathy, R.K., Bhattacharyya, A., Pachori, R.B. (2019). A novel approach for detection of myocardial infarction from ECG signals of multiple electrodes. IEEE Sensors Journal, 19(12): 4509-4517. https://doi.org/10.1109/JSEN.2019.2896308

[12] Baloglu, U.B., Talo, M., Yildirim, O., San Tan, R., Acharya, U.R. (2019). Classification of myocardial infarction with multi-lead ECG signals and deep CNN. Pattern Recognition Letters, 122: 23-30. https://doi.org/10.1016/j.patrec.2019.02.016

[13] Sridhar, C., Lih, O.S., Jahmunah, V., Koh, J.E., Ciaccio, E.J., San, T.R., Arunkumar, N., Kadry, S., Rajendra Acharya, U. (2021). Accurate detection of myocardial infarction using non linear features with ECG signals. Journal of Ambient Intelligence and Humanized Computing, 12: 3227-3244. https://doi.org/10.1007/s12652-020-02536-4

[14] Jahmunah, V., Ng, E.Y.K., San, T.R., Acharya, U.R. (2021). Automated detection of coronary artery disease, myocardial infarction and congestive heart failure using Gabor CNN model with ECG signals. Computers in Biology and Medicine, 134: 104457. https://doi.org/10.1016/j.compbiomed.2021.104457

[15] Fatimah, B., Singh, P., Singhal, A., Pramanick, D., Pranav, S., Pachori, R.B. (2021). Efficient detection of myocardial infarction from single lead ECG signal. Biomedical Signal Processing and Control, 68: 102678. https://doi.org/10.1016/j.bspc.2021.102678

[16] Kapfo, A., Dandapat, S., Kumar Bora, P. (2020). Automated detection of myocardial infarction from ECG signal using variational mode decomposition based analysis. Healthcare Technology Letters, 7(6): 155-160. https://doi.org/10.1049/htl.2020.0015

[17] Cho, Y., Kwon, J.M., Kim, K.H., Medina-Inojosa, J.R., Jeon, K.H., Cho, S., Lee, S.Y., Park, J., Oh, B.H. (2020). Artificial intelligence algorithm for detecting myocardial infarction using six-lead electrocardiography. Scientific Reports, 10(1): 20495. https://doi.org/10.1038/s41598-020-77599-6

[18] Kayikcioglu, I., Akdeniz, F., Köse, C., Kayikcioglu, T. (2020). Time-frequency approach to ECG classification of myocardial infarction. Computers & Electrical Engineering, 84: 106621. https://doi.org/10.1016/j.compeleceng.2020.106621

[19] Zhao, Y., Xiong, J., Hou, Y., Zhu, M., Lu, Y., Xu, Y., Teliewubai, J., Liu, W., Xu, X., Li, X., Liu, Z., Peng, W., Zhao, X., Zhang, Y., Xu, Y. (2020). Early detection of ST-segment elevated myocardial infarction by artificial intelligence with 12-lead electrocardiogram. International Journal of Cardiology, 317: 223-230. https://doi.org/10.1016/j.ijcard.2020.04.089

[20] Hammad, M., Chelloug, S.A., Alkanhel, R., Prakash, A. J., Muthanna, A., Elgendy, I.A., Pławiak, P. (2022). Automated detection of myocardial infarction and heart conduction disorders based on feature selection and a deep learning model. Sensors, 22(17): 6503. https://doi.org/10.3390/s22176503

[21] Rai, H.M., Chatterjee, K. (2022). Hybrid CNN-LSTM deep learning model and ensemble technique for automatic detection of myocardial infarction using big ECG data. Applied Intelligence, 52(5): 5366-5384. https://doi.org/10.1007/s10489-021-02696-6

[22] Han, C., Pan, S., Que, W., Wang, Z., Zhai, Y., Shi, L. (2022). Automated localization and severity period prediction of myocardial infarction with clinical interpretability based on deep learning and knowledge graph. Expert Systems with Applications, 209: 118398. https://doi.org/10.1016/j.eswa.2022.118398

[23] Muraki, R., Teramoto, A., Sugimoto, K., Sugimoto, K., Yamada, A., Watanabe, E. (2022). Automated detection scheme for acute myocardial infarction using convolutional neural network and long short-term memory. PloS One, 17(2): e0264002. https://doi.org/10.1371/journal.pone.0264002

[24] Mirza, A.H., Nurmaini, S., Partan, R.U. (2022). Automatic classification of 15 leads ECG signal of myocardial infarction using one dimension convolutional neural network. Applied Sciences, 12(11): 5603. https://doi.org/10.3390/app12115603

[25] Wagner, P., Strodthoff, N., Bousseljot, R., Samek, W., Schaeffter, T. (2022). PTB-XL, a large publicly available electrocardiography dataset (version 1.0.3). PhysioNet. https://doi.org/q0.13026/kfzx-aw45

[26] Huang, N.E., Shen, Z., Long, S.R., Wu, M.C., Shih, H.H., Zheng, Q., Yen, N.C., Tung, C.C., Liu, H.H. (1998). The empirical mode decomposition and the Hilbert spectrum for nonlinear and non-stationary time series analysis. Proceedings of the Royal Society of London. Series A: Mathematical, Physical and Engineering Sciences, 454(1971): 903-995. https://doi.org/10.1098/rspa.1998.0193

[27] Hasan, N.I., Bhattacharjee, A. (2019). Deep learning approach to cardiovascular disease classification employing modified ECG signal from empirical mode decomposition. Biomedical Signal Processing and Control, 52: 128-140. https://doi.org/10.1016/j.bspc.2019.04.005

[28] Liu, J., Zhang, C., Zhu, Y., Ristaniemi, T., Parviainen, T., Cong, F. (2020). Automated detection and localization system of myocardial infarction in single-beat ECG using Dual-Q TQWT and wavelet packet tensor decomposition. Computer Methods and Programs in Biomedicine, 184: 105120. https://doi.org/10.1016/j.cmpb.2019.105120

[29] Kumar, A., Tomar, H., Mehla, V.K., Komaragiri, R., Kumar, M. (2021). Stationary wavelet transform based ECG signal denoising method. ISA Transactions, 114: 251-262. https://doi.org/10.1016/j.isatra.2020.12.029

[30] Chakraborty, A., Chatterjee, S., Majumder, K., Shaw, R.N., Ghosh, A. (2022). A comparative study of myocardial infarction detection from ECG data using machine learning. In Advanced Computing and Intelligent Technologies: Proceedings of ICACIT 2021, Springer Singapore, pp. 257-267. https://doi.org/10.1007/978-981-16-2164-2_21

[31] Kora, P., Abraham, A., Meenakshi, K. (2020). Heart disease detection using hybrid of bacterial foraging and particle swarm optimization. Evolving Systems, 11(1): 15-28. https://doi.org/10.1007/s12530-019-09312-6

[32] Atal, D.K., Saroha, J. (2017). A fuzzy PSO clustering with decision tree based expert system for ECG signal analysis and classification. International Journal of Computer Science & Communication, 9(1): 279-291.

[33] Qamar, S. (2022). ECG signal processing by feature selection with classification based on machine learning architectures in cardiovascular disease detection. Research Square. https://doi.org/10.21203/rs.3.rs-1953217/v1

[34] Zhang, G., Si, Y., Wang, D., Yang, W., Sun, Y. (2019). Automated detection of myocardial infarction using a Gramian angular field and principal component analysis network. IEEE Access, 7: 171570-171583. https://doi.org/10.1109/ACCESS.2019.2955555

[35] Jafarian, K., Vahdat, V., Salehi, S., Mobin, M. (2020). Automating detection and localization of myocardial infarction using shallow and end-to-end deep neural networks. Applied Soft Computing, 93: 106383. https://doi.org/10.1016/j.asoc.2020.106383

[36] Dey, M., Omar, N., Ullah, M.A. (2021). Temporal feature-based classification into myocardial infarction and other CVDS merging CNN and bi-LSTM from ECG signal. IEEE Sensors Journal, 21(19): 21688-21695. https://doi.org/10.1109/JSEN.2021.3079241

[37] Wasimuddin, M., Elleithy, K., Abuzneid, A., Faezipour, M., Abuzaghleh, O. (2021). Multiclass ECG signal

analysis using global average-based 2-D convolutional neural network modeling. Electronics, 10(2): 170. https://doi.org/10.3390/electronics10020170

[38] Feng, K., Pi, X., Liu, H., Sun, K. (2019). Myocardial infarction classification based on convolutional neural network and recurrent neural network. Applied Sciences, 9(9): 1879. https://doi.org/10.3390/app9091879

[39] He, Z., Yuan, Z., An, P., Zhao, J., Du, B. (2021). MFB-LANN: A lightweight and updatable myocardial infarction diagnosis system based on convolutional neural networks and active learning. Computer Methods and Programs in Biomedicine, 210: 106379. https://doi.org/10.1016/j.cmpb.2021.106379

[40] Xiao, R., Xu, Y., Pelter, M.M., Fidler, R., Badilini, F., Mortara, D.W., Hu, X. (2018). Monitoring significant ST changes through deep learning. Journal of Electrocardiology, 51(6): S78-S82. https://doi.org/10.1016/j.jelectrocard.2018.07.026

[41] Liu, W., Huang, Q., Chang, S., Wang, H., He, J. (2018). Multiple-feature-branch convolutional neural network for myocardial infarction diagnosis using electrocardiogram. Biomedical Signal Processing and Control, 45: 22-32. https://doi.org/10.1016/j.bspc.2018.05.013

[42] Hao, P., Gao, X., Li, Z., Zhang, J., Wu, F., Bai, C. (2020). Multi-branch fusion network for Myocardial infarction screening from 12-lead ECG images. Computer Methods and Programs in Biomedicine, 184: 105286. https://doi.org/10.1016/j.cmpb.2019.105286

[43] Gumpfer, N., Grün, D., Hannig, J., Keller, T., Guckert, M. (2021). Detecting myocardial scar using electrocardiogram data and deep neural networks. Biological Chemistry, 402(8): 911-923. https://doi.org/10.1515/hsz-2020-0169

[44] Zhang, G., Si, Y., Yang, W., Wang, D. (2020). A robust multilevel dwt densely network for cardiovascular disease classification. Sensors, 20(17): 4777. https://doi.org/10.3390/s20174777

[45] Yadav, S.S., More, S.B., Jadhav, S.M., Sutar, S.R. (2021). Convolutional neural networks based diagnosis of myocardial infarction in electrocardiograms. In 2021 International Conference on Computing, Communication, and Intelligent Systems (ICCCIS), Greater Noida, India, pp. 581-586. https://doi.org/10.1109/ICCCIS51004.2021.9397193

[46] Gupta, A., Huerta, E., Zhao, Z., Moussa, I. (2021). Deep learning for cardiologist-level myocardial infarction detection in electrocardiograms. In 8th European Medical and Biological Engineering Conference: Proceedings of the EMBEC 2020, November 29-December 3, 2020 Portorož, Slovenia. Springer International Publishing.Springer, Cham, pp. 341-355. https://doi.org/10.1007/978-3-030-64610-3_40

[47] Jikui, L., Ruxin, W., Bo, W., Zengding, L., Fen, M., Ye, L.I. (2021). Myocardial infarction detection and localization with electrocardiogram based on convolutional neural network. Chinese Journal of Electronics, 30(5): 833-842. https://doi.org/10.1049/cje.2021.06.005